Theoretical investigations of novel Janus Pb_2SSe monolayer as a potential multifunctional material for piezoelectric, photovoltaic and thermoelectric applications

Fusheng Zhang,[1] Jian Qiu,[2] Haojie Guo,[1] Lingmei Wu,[1] Bao Zhu,[2] Kai Zheng,[1] Hui Li,[1] Zeping Wang,[1] Xianping Chen*[1] and Jiabing Yu*[1]

[1]*Key Laboratory of Optoelectronic Technology & Systems, Education Ministry of China, and College of Optoelectronic Engineering, State Key Laboratory of Power Transmission Equipment & System Security and New Technology, Chongqing University, Chongqing 400044, China; orcid.org/0000-0002-2461-4010.*

[2]*Faculty of Mechanical and Electrical Engineering, Guilin University of Electronic Technology, Guilin 541004, China.*

**Corresponding author (Email: xianpingchen@cqu.edu.cn and yujiab@cqu.edu.cn)*

Bonding properties

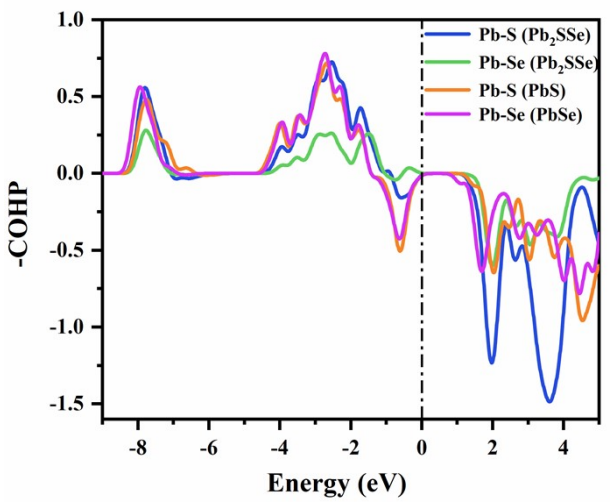

Fig. S1. The normalized COHP for Pb-S and Pb-Se in Pb_2SSe monolayer and Pb-S for PbS monolayer and Pb-Se monolayer.

Table S1. ICOHP (eV) for different bond interactions with Pb_2SSe, PbS and PbSe monolayer.

phase	Pb-S (Pb_2SSe)	Pb-Se (Pb_2SSe)	Pb-S (PbS)	Pb-Se (PbSe)
ICOHP	-2.92	-1.21	-2.11	-2.13

Thermodynamic stability

The formation energy of a 2D material can be obtained by the following equation:[1]

$$\Delta E_{\mathrm{f}} = \frac{E_{2D}}{N_{2D}} - \frac{E_{3D}}{N_{3D}} \tag{S1}$$

where E_{2D} and E_{3D} represent the energies of the monolayer and bulk material, respectively, and N_{2D} and N_{3D} are the numbers of atoms in the respective unit cells. The energy above hull can be described by the formation enthalpy (ΔH) of 2D Pb_2SSe using the relation: [2]

$$\Delta H_{Pb_2SSe} = E_{Pb_2SSe} - [xE_{PbS} + (1-x)E_{Se}] \tag{S2}$$

in which E_{Pb_2SSe} and E_{PbS} are the energy of Pb_2SSe and PbS monolayers, and E_{Se} represents the energy of pure Se element.

Mechanical stability

Table S2. Calculated Elastic Stiffness Constants *C* (N/m) of Pb_2SSe monolayer.

system	C_{11}	C_{12}	C_{22}	C_{44}	Status
Pb_2SSe	34.1	20.9	46.5	16.9	stable

The mechanical stability of Pb_2SSe monolayer has been verified by the satisfaction of Born criterion:

$$C_{11} > 0,\ C_{22} > 0,\ C_{44} > 0,\ C_{11}C_{22} > C_{12}^2$$

Young's modulus and Poisson's ratio:

The angle-dependent Young's modulus Y(θ) and Poisson's ratio v(θ) can be computed using the following formula:

$$Y(\theta) = \frac{C_{11}C_{22} - C_{12}^2}{C_{11}s^4 + C_{22}c^4 + (\frac{C_{11}C_{22} - C_{12}^2}{C_{66}} - 2C_{12})c^2s^2} \quad \text{(S3)}$$

$$v(\theta) = \frac{C_{12}(c^4 + s^4) - (C_{11} + C_{22} - \frac{C_{11}C_{22} - C_{12}^2}{C_{66}})c^2s^2}{C_{11}s^4 + C_{22}c^4 + (\frac{C_{11}C_{22} - C_{12}^2}{C_{66}} - 2C_{12})c^2s^2} \quad \text{(S4)}$$

where *c* and s represent $\cos\theta$ and $\sin\theta$, respectively.

Computation of power conversion efficiency (PCE) and optical absorption coefficient

The optical absorption coefficients of both monolayers and heterostructures were calculated from the frequency-dependent dielectric function, ε(ω), using the following formula:

$$\alpha(\omega)=\sqrt{2}\omega[\sqrt{\varepsilon_1^2(\omega)+\varepsilon_2^2(\omega)}-\varepsilon_1(\omega)]^{1/2} \quad \text{(S5)}$$

in which $\varepsilon_1(\omega)$ and $\varepsilon_2(\omega)$ are the real and imaginary part of the complex dielectric function.

The power conversion efficiency (PCE) of Pb_2SSe/SnSe and Pb_2SSe/GeSe vdW heterostructure can be expressed by[3]

$$\eta=\frac{\beta_{FF}V_{OC}J_{SC}}{P_{solar}}=\frac{0.65(E_g^d-\Delta E_c-0.3)\int_{E_g^d}^{\infty}P(\mathrm{h}\omega)d(\mathrm{h}\omega)}{\int_0^{\infty}P(\mathrm{h}\omega)d(\mathrm{h}\omega)} \quad \text{(S6)}$$

where P_{solar} is the total incident solar radiation, $P(\mathrm{h}\omega)$ is the AM 1.5 solar energy flux in units of $Wm^{-2}eV^{-1}$ and $\mathrm{h}\omega$ is the photo energy. β_{FF} is the fill factor, equaling to 0.65. V_{OC}=$E_g^d-\Delta E_c-0.3$ represents the maximum open-circuit voltage, where E_g^d is the donor band gap and ΔE_c is the conduction band offset.

The temperature- and doping-dependent electrical transport properties

$$n_h(T,\mu)=\frac{2}{P}\iint_{BZ}[1-f_0(T,\varepsilon,\mu)D(\varepsilon)]d\varepsilon \quad \text{(S7)}$$

$$n_e(T,\mu)=\frac{2}{P}\iint_{BZ}f_0(T,\varepsilon,\mu)D(\varepsilon)d\varepsilon \quad \text{(S8)}$$

$$S_{\alpha\beta}(T,\mu)=\frac{1}{eTP\sigma_{\alpha\beta}(T,\mu)}\int\bar{\sigma}_{\alpha\beta}(\varepsilon)(\varepsilon-\mu)[-\frac{\partial f_0(T,\varepsilon,\mu)}{\partial\varepsilon}]d\varepsilon \quad \text{(S9)}$$

$$\sigma_{\alpha\beta}(T,\mu)=\frac{2}{P}\int\bar{\sigma}_{\alpha\beta}(\varepsilon)[-\frac{\partial f_0(T,\varepsilon,\mu)}{\partial\varepsilon}]d\varepsilon \quad \text{(S10)}$$

$$\kappa_{\alpha\beta}^e(T,\mu)=\frac{1}{e^2TP}\int\bar{\sigma}_{\alpha\beta}(\varepsilon)(\varepsilon-\mu)^2[-\frac{\partial f_0(T,\varepsilon,\mu)}{\partial\varepsilon}]d\varepsilon \quad \text{(S11)}$$

where P is the volume of the unit cell, f_0 is the Fermi-Dirac distribution, μ represents the chemical potential, $D(\varepsilon)$ is the density of states, $\bar{\sigma}_{\alpha\beta}(\varepsilon)$ is the energy dependent conductivity tensor.

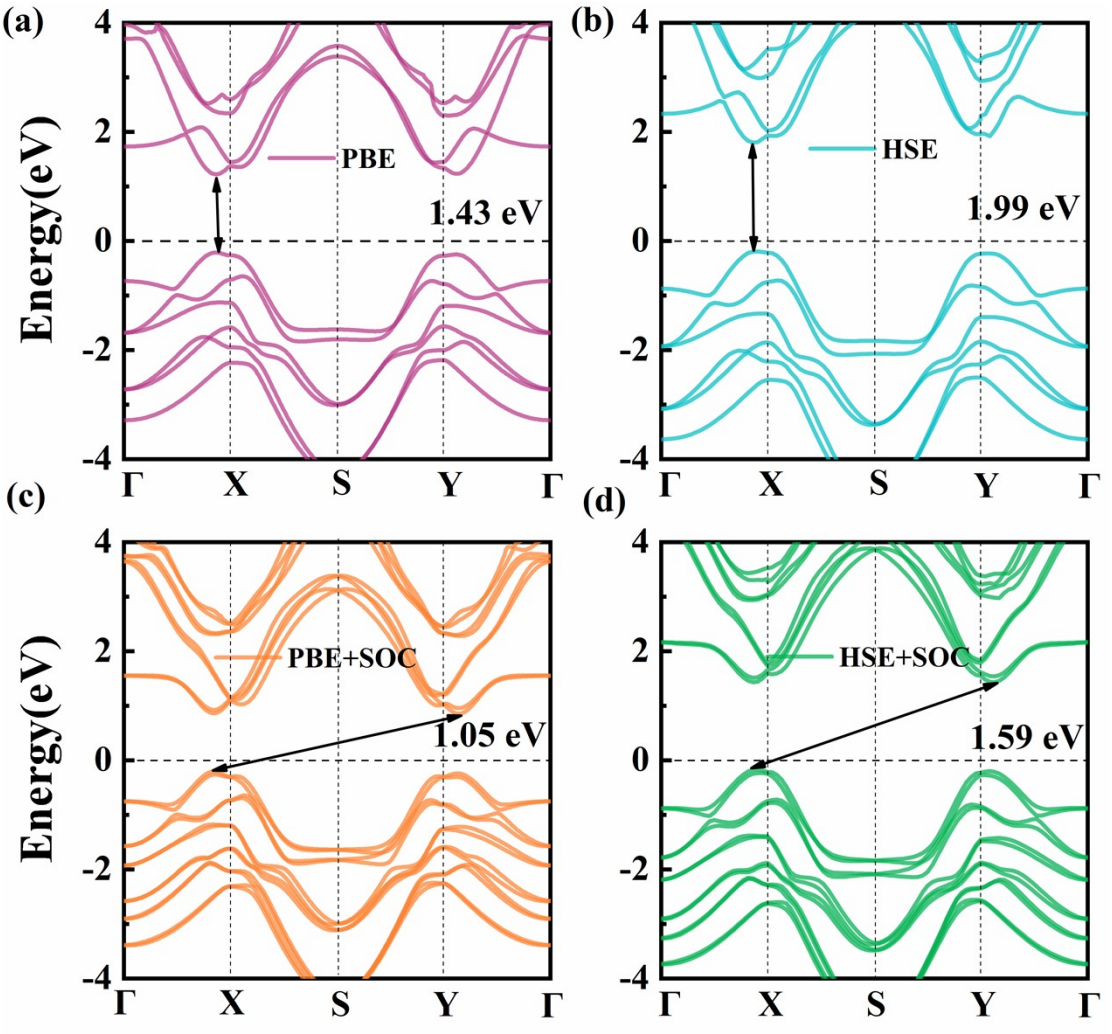

Fig. S2. The electronic band structures of monolayer Pb_2SSe calculated at the (a) PBE and HSE06, (b) PBE+SOC and HSE06+SOC level, respectively.

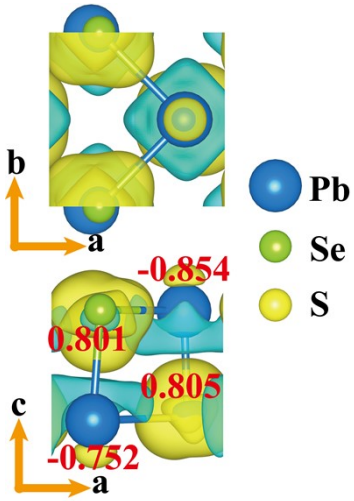

Fig. S3. Views along c direction and along b direction of charge density difference for Pb2SSe monolayer.

Table S3. The lattice constants (*a* and *b*) Å, interlayer distances (*d*) Å and interlayer binding energy (E_b) meV/Å^2 of bilayer Pb_2SSe.

Structure	*a* (Å)	*b* (Å)	*d* (Å)	E_b (meV/ Å^2)
(a)	4.349	4.307	3.32	-81.21
(b)	4.386	4.278	3.87	-78.22
(c)	4.319	4.342	3.72	-79.06
(d)	4.351	4.309	3.69	-68.79

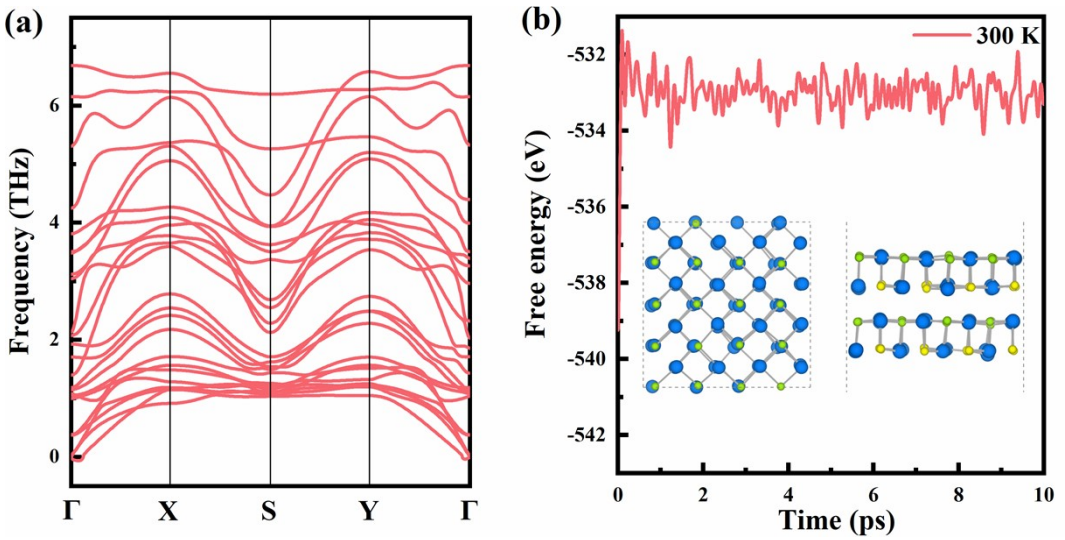

Fig. S4. (a) Phonon spectrum of Pb_2SSe bilayers. (b) Free energy fluctuation and final structures in AIMD simulation at 300 K.

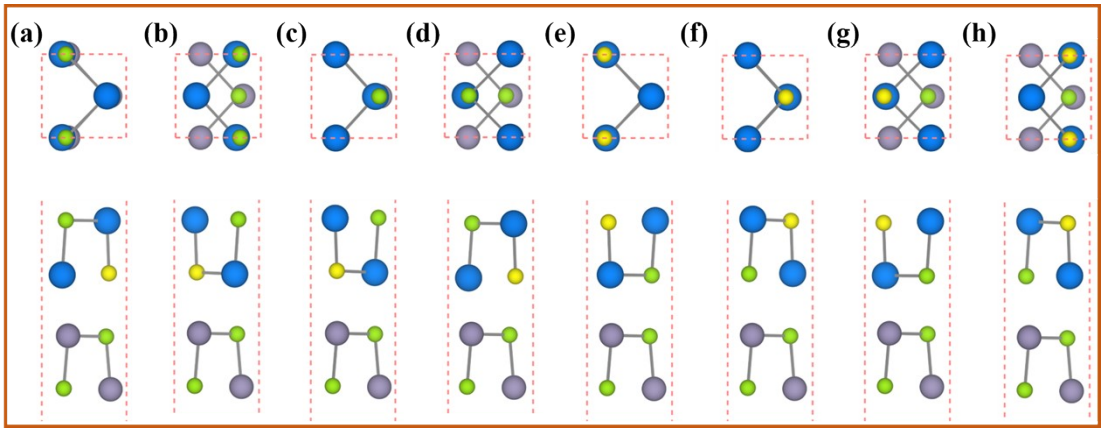

Fig. S5. (a-h) The structure of different stacking patterns of the Pb_2SSe/SnSe and Pb_2SSe/GeSe heterostructures.

Table S4. The lattice constants (a and b) Å, interlayer distances (d) Å and interlayer binding energy (E_b) meV/Å^2 of the Pb_2SSe/SnSe and Pb_2SSe/GeSe heterostructures.

Structure	a	b	d	E_b
SnSe	4.397	4.294		
GeSe	4.289	3.974		
a	4.422	4.266	3.642	-25.73
b	4.425	4.264	3.826	-25.72
c	4.430	4.274	3.450	-27.18
d	4.359	4.288	3.357	-24.47
e	4.394	4.293	3.578	-26.74
f	4.403	4.282	3.329	-25.86
g	4.387	4.287	3.620	-18.11
h	4.440	4.269	3.762	-26.63
A	4.375	4.114	3.452	-13.71
B	4.409	4.111	3.456	-21.28
C	4.408	4.110	3.446	-21.30
D	4.406	4.109	3.742	-20.14
E	4.373	4.120	3.519	-21.27
F	4.379	4.112	3.509	-14.24
G	4.373	4.121	3.357	-20.47
H	4.402	4.110	3.754	-20.82

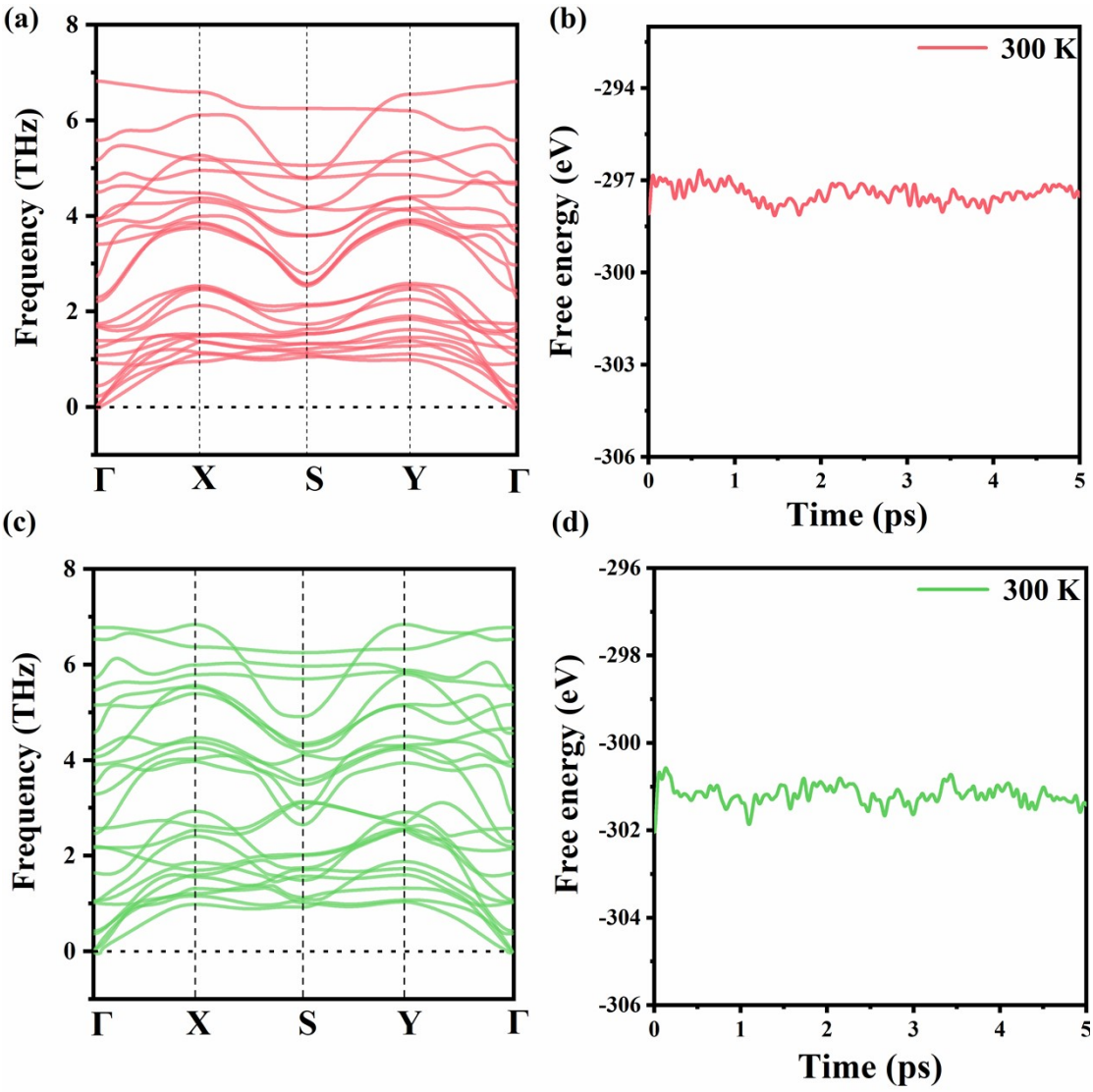

Fig. S6. (a) and (c) Phonon spectrum of Pb_2SSe/SnSe and Pb_2SSe/GeSe heterostructures. (b) and (d) Free energy fluctuation and final structures in AIMD simulation at 300 K for Pb_2SSe/SnSe and Pb_2SSe/GeSe heterostructures.

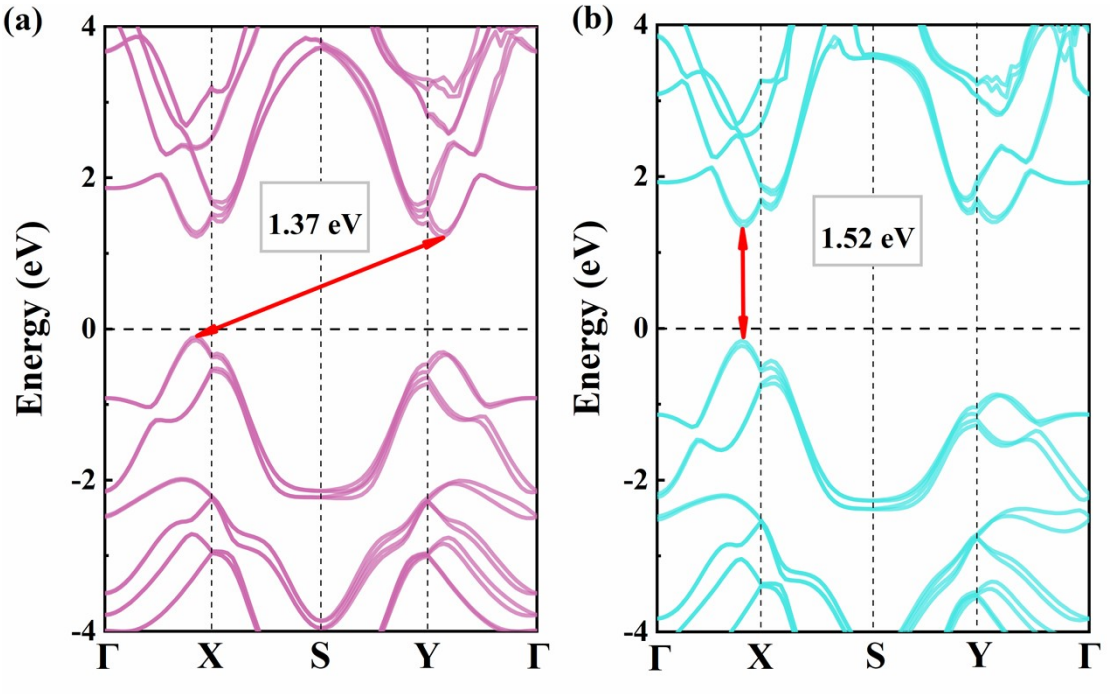

Fig. S7. (a) and (b) The band structures of SnSe and GeSe monolayers using HSE06 functional with consideration of SOC effect.

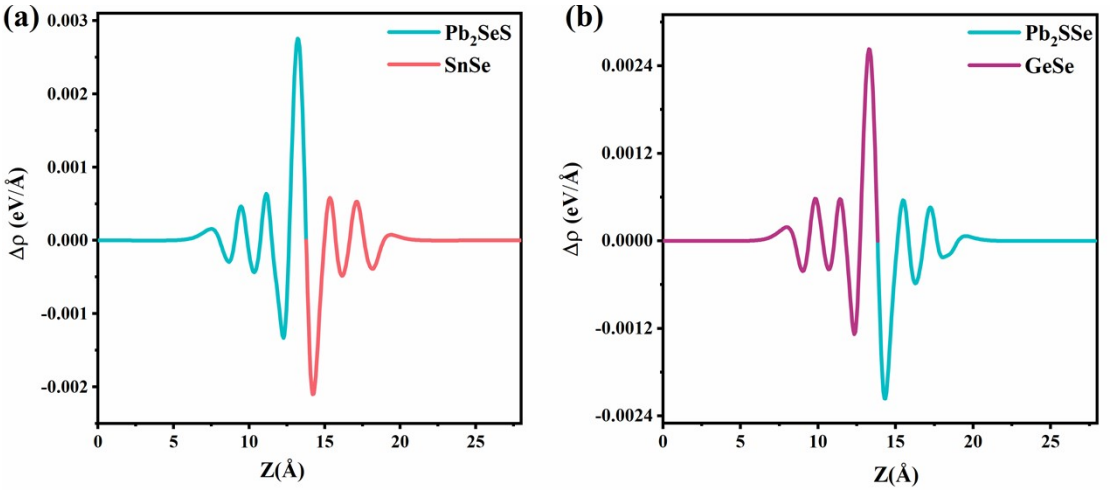

Fig. S8. (a) and (b) Plane averaged charge density difference of Pb_2SSe/SnSe and Pb_2SSe/GeSe heterostructures, respectively.

Table S5. The calculated work functions of the monolayers and heterostructures.

System	SnSe	GeSe	Pb_2SSe	Pb_2SSe/SnSe	Pb_2SSe/GeSe
Work function	4.28	4.36	4.33	4.24	4.30

Table S6. The Calculated effective mass (m^*), Elastic Moduli (C), Deformation potentials (E_d), carrier mobility and carrier relaxation time of monolayer Pb_2SSe along x and y directions.

Material	direction	Carrier type	m^*/m_0	C (N m^{-1})	E_d (eV)	μ (cm^{2}V^{-1}s^{-1})
Pb_2SSe/SnSe	x	e	0.22	39.8	0.39	77292
		h	0.38	39.8	3.82	270
	y	e	0.17	78.7	4.39	2020
		h	0.25	78.7	7.65	308
Pb_2SSe/GnSe	x	e	0.20	46.7	1.49	7530
		h	0.39	46.7	7.31	82
	y	e	0.24	80.3	1.86	5754
		h	0.22	80.3	5.54	773

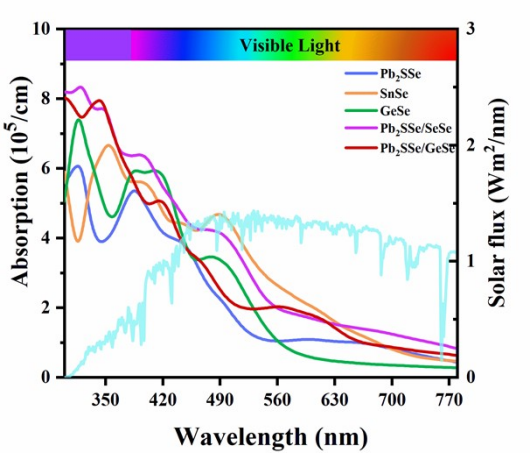

Fig. S9. The optical absorption spectrum of the monolayer Pb_2SSe, SnSe, GeSe Pb_2SSe/SnSe and Pb_2SSe/GeSe heterostructures along y direction.

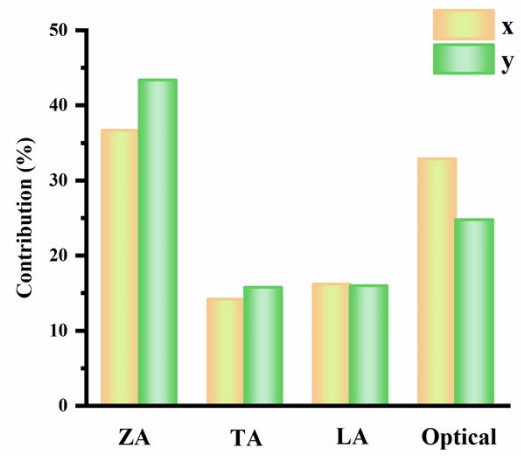

Fig. S10. Phonon modes (ZA, TA, LA and Optical) contributions towards the total κ_L at 300 K along x and y directions for the Pb_2SSe monolayer.

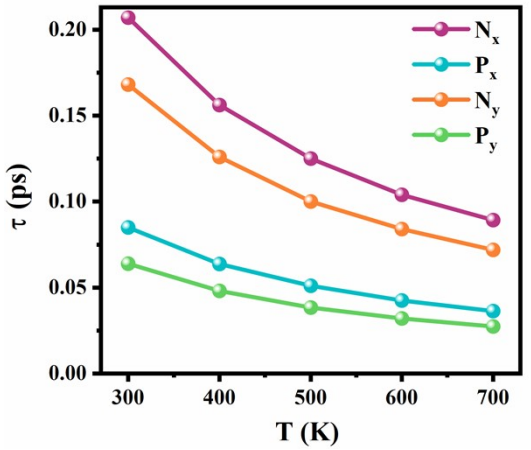

Fig. S11. The temperature dependence of relaxation time (τ) for p- and n-type doping along x and y directions.

Reference

1. A. K. Singh, K. Mathew, H. L. Zhuang and R. G. Hennig, *J. of Phys. Chem. Lett.*, 2015, **6**, 1087-1098.
2. Y. H. Robin Chang, T. L. Yoon, K. H. Yeoh and T. L. Lim, *Int. J. Energy Res.* 2021, **45**, 2085-2099.
3. J. Dai and X. C. Zeng, *J. Phys. Chem. Lett.*, 2014, **5**, 1289-1293.